

# Theoretical Model of the *n*-Propylbenzene Formation in the Benzene Isopropylation over Zeolites. An Anti-Markovnikov-Type Proton Addition Promoted by the Steric Effect of MFI and MEL Zeolite Channels

Judit Šponer,\* Jiří Šponer, Jiří Čejka, and Blanka Wichterlová

*J. Heyrovský Institute of Physical Chemistry, Academy of Sciences of the Czech Republic, Dolejškova 3, 182 23 Prague 8, Czech Republic*

*Received: January 6, 1998; In Final Form: April 15, 1998*

Proton-catalyzed bimolecular reaction of isopropylbenzene with benzene leading to *n*-propylbenzene was studied employing ab initio quantum chemical calculations. The reaction complex was described by a complex of protonated isopropylbenzene and the benzene molecule. Geometry optimizations were performed at the Hartree–Fock level of theory under two conditions: (i) full relaxation of the geometrical parameters, reflecting the situation in nonrestricted reaction space; and (ii) imposing geometrical constraints, representing the steric conditions at the channel intersection in zeolites of the MFI and MEL structural types. Computations on the fully relaxed complex of protonated isopropylbenzene and benzene showed that *n*-propylbenzene formation cannot be expected on catalysts with nonrestricted reaction space. Use of the constrained model verified existence of a reaction pathway leading to *n*-propylbenzene formation, in agreement with the experimental observation.

## Introduction

Isopropylation of benzene and toluene over zeolite-based catalysts has attracted considerable interest as a challenge for the replacement of harmful AlCl<sub>3</sub> or supported H<sub>3</sub>PO<sub>4</sub> that are used in current technological processes.<sup>1</sup> When medium-pore zeolites<sup>2</sup> (namely, MFI and MEL structures) were used, a mixture of both iso- and *n*-propylbenzene and propyltoluene isomers was observed. On the other hand, over catalysts with “open surfaces” (AlCl<sub>3</sub> or H<sub>3</sub>PO<sub>4</sub>), almost exclusively iso-isomers were obtained. The first reaction step resulted in formation of isopropylaromatics, which is in agreement with the well-known higher stability of the secondary carbocations in contrast to the primary carbocations. It has been found that *n*-propylbenzene — the main byproduct of the isopropylation process — is formed in a subsequent reaction step via the proton-catalyzed isomerization of the isopropylbenzene formed in the first reaction step. A monomolecular mechanism of the isomerization of iso- to *n*-propyltoluene was proposed by Fraenkel and Levy,<sup>2</sup> whereas a bimolecular mechanism of *n*-propylbenzene formation in an excess of benzene was suggested by Beyer and Borbély.<sup>3</sup> A <sup>13</sup>C magic angle spinning (MAS) NMR study<sup>4,5</sup> on the transalkylation reaction between labeled isopropylbenzene and benzene reactants has unambiguously evidenced the bimolecular mechanism. A kinetic study of the reaction between toluene and isopropylbenzene, yielding *n*-propyltoluene and benzene with isopropyltoluene and resulting in *n*-propylbenzene formation over MFI, provided further support for the bimolecular mechanism.<sup>6</sup> Thus, based on the experimental results, a two-step reaction mechanism has been proposed for the propylation of monoaromatics leading to iso- and *n*-propyl derivatives.

The dramatic effect of the inner geometry and architecture of the zeolite channels on the iso- to *n*-propylbenzene and iso- to *n*-propyltoluene composition in the products was reported by Čejka et al.<sup>7,8</sup> In these experiments, the main product of the alkylation reaction over zeolite of the MFI structural type

is *n*-propylbenzene. In comparison, with zeolites exhibiting more “open” three-dimensional structures, such as type FAU or BEA, significantly less or no *n*-propyltoluenes were formed. The monodimensional MOR structure did not exhibit any activity in the transalkylation reaction and only isopropyltoluenes were found in the products. Therefore, we concluded that the narrow perpendicular intersecting channels present in zeolites of MFI and MEL structures provide optimum geometrical conditions for *n*-propylbenzene formation. This effect was termed “structure-directed transition state selectivity.”

In addition to the steric effect of the zeolite architecture, acid site strengths and their number affect the rate of the transalkylation reaction and thus the ratio of iso- and *n*-propyltoluenes in the product. This effect has been shown for the propylation of toluene over MFI structures with isomorphous substitution of Al, Fe, and In in the silicate framework.<sup>9</sup> This work provided evidence that the transalkylation step requires proton transfer from the zeolite to the reaction complex.

Experimental investigations on the adsorption of benzene over the acidic form of MFI<sup>10,11</sup> show that at room temperature, benzene forms only a weak hydrogen bond with the zeolitic OH group, and, thus is not protonated. A detailed in situ infrared (IR) spectroscopic study on the adsorption and isomerization of xylene over MFI<sup>12</sup> reveals, however, that the spectra exhibit strong temperature dependence. Therefore, though up to now no direct experimental evidence is available, under the reaction conditions (520 K), proton transfer from the zeolite to the reaction center can be assumed. On the other hand, a proton-catalyzed transalkylation reaction (that requires two reactants) is hardly possible without transfer of a proton from the zeolite to the reactant, because the zeolitic proton basically replaces the leaving alkyl group of the alkyl-donor reactant. Therefore, as a starting point in our computations, we assumed formation of protonated isopropylbenzene molecules.

In general, theoretical studies on the chemistry of the zeolitic protons are well documented in the literature.<sup>13–15</sup> Reactivity

and stability of carbocation-type species in zeolite matrixes has been addressed by numerous experimental and theoretical investigations.<sup>16–20</sup> Gas-phase mass spectrometric investigations combined with quantum chemical calculations<sup>21,22</sup> have shown that protonated isopropylbenzene molecules can be stabilized as ion-neutral complexes in two different ways, expressed by the following formulas:  $[\text{C}_6\text{H}_6\cdot\text{iso-C}_3\text{H}_7^+]$  (cation **a**) and  $[\text{C}_6\text{H}_7^+\cdot\text{C}_3\text{H}_6]$  (cation **b**). Although cation **a** represents a lower energy form of the protonated isopropylbenzene isomers, cation **b** (a complex of the arenium–alkene type) offers a more appropriate model to describe the proton shift within the propylene part. Therefore, in our model we considered a complex of cation **b** and benzene and determined possible reaction pathways of the transalkylation reaction following the displacement of the bridging hydrogen of cation **b** toward the propylene part.

It is reasonable to assume that the transalkylation reaction between isopropylbenzene and benzene molecules takes place in the channel intersections of the MFI structure, because this reaction does not occur in the monodimensional channels of the MOR structure. According to a theoretical approach mentioned under the name “*molecular traffic control*,”<sup>23</sup> the molecules adsorbed at the channel intersections of the MFI structure are especially suitable targets for attacks by reactant molecules from the direction of the sinusoidal channels. The primary aim of our study is to describe the isomerization reaction<sup>4–6</sup> between benzene and isopropylbenzene leading to *n*-propylbenzene, so we took into consideration the main effect of the MFI and MEL channels (i.e., their perpendicularity, with geometrical constraints). Therefore, we assumed that the protonated isopropylbenzene molecule (represented by cation **b**) is adsorbed at the channel intersection in zeolites of MFI or MEL structural type and undergoes an attack by the reactant benzene molecule approaching through the sinusoidal channel. To explain the role of the perpendicularity of the intersecting channels on the rate of the isomerization, comparative computations were performed on the fully relaxed complex of cation **b** and benzene as well.

In this study, a complex composed by cation **b** and benzene is investigated using ab initio quantum chemical calculations with respect to its potential participation in the isomerization reaction. Beyond the mechanism of the *n*-propylbenzene formation, this study addresses the operation of the phenomenon postulated as “*structure-directed transition state selectivity*”.

## Computations

Several sets of calculations were carried out.

First, geometries of all complexes were optimized within the Hartree–Fock (HF) approximation with the 6-31G\*\* basis set of atomic orbitals. Analytic gradients were computed following the Berny-algorithm.<sup>24</sup> In several cases, analytic second derivatives had to be used to obtain optimized structures. We studied initial and final structures of the expected chemical process and a number of structures where the C···H distance was fixed along the proposed reaction pathway. The energy difference between two structures is evaluated as a difference between their total HF/6-31G\*\* electronic energies (designated as  $E^{\text{tot}}$  throughout this paper). This value contains all intramolecular and intermolecular energy contributions with the exception of the dispersion attraction, which is neglected at the HF level. The dispersion attraction originates in an intermolecular electron correlation. However, because of the size of the system, we could not apply any post-HF technique including the electron correlation effects for the optimizations. (Let us emphasize that

the Density Functional Theory ignores the dispersion attraction as does the HF theory and is, therefore, not recommended for molecular clusters.<sup>25,26</sup>) We believe that although the dispersion effects are important for the present system, the gradient optimization made at the HF level provides reasonable intermolecular geometries because the system is dominated by the electrostatic contributions and induction effects, which are characteristic of ionic complexes. Furthermore, the gradient optimization is inherently not corrected for the basis set superposition error, which partly compensates for the neglect of dispersion attraction.

Next, to estimate the effect of dispersion energy on the intermolecular stabilization of various complexes we evaluated the intermolecular interaction energies using the second-order Møller–Plesset (MP2) perturbational theory. The standard 6-31G basis set augmented by one set of diffuse (momentum-optimized; exponent of 0.25) *d*-polarization functions was used. These calculations were made as single-point energy calculations using the HF/6-31G\*\*-optimized geometries, which is abbreviated as the MP2/6-31G\*(0.25)//HF/6-31G\*\* level. The use of diffuse polarization functions improves the dispersion attraction significantly.<sup>27–29</sup> Recent studies on small aromatic dimers indicate that the MP2/6-31G\*(0.25) interaction energies are surprisingly close to the actual values.<sup>30,31</sup>

The interaction energy of a trimer ( $\Delta E^{\text{ABC}}$ ) is expressed in the following way:  $\Delta E^{\text{ABC}} = E^{\text{ABC}} - E^{\text{A}} - E^{\text{B}} - E^{\text{C}} = \Delta E^{\text{AB}} + \Delta E^{\text{AC}} + \Delta E^{\text{BC}} + \Delta E^3$  (see ref 32), where  $E^{\text{ABC}}$ ,  $E^{\text{A}}$ ,  $E^{\text{B}}$ , and  $E^{\text{C}}$  are the electronic energies of the trimer and the monomers, respectively,  $\Delta E^{\text{AB}}$ ,  $\Delta E^{\text{AC}}$ , and  $\Delta E^{\text{BC}}$  are the pair interaction energies of the corresponding dimers, and  $\Delta E^3$  is the three-body term. All contributions consist of HF ( $E^{\text{HF}}$ ) and correlation ( $E^{\text{cor}}$ ) parts and were corrected for the basis set superposition error using standard counterpoise procedure in a trimer-centered basis set.

The MP2/6-31G\*(0.25)//HF/6-31G\*\* interaction energies can be used to rationalize the effect of intermolecular interactions for stabilization of various complexes involved in the studied process. Nevertheless, for the evaluation of the reaction mechanism, the HF/6-31G\*\* total electronic energies is preferred.<sup>33</sup>

All ab initio quantum chemical calculations were carried out using the Gaussian 94 computer code.<sup>34</sup> The zero-point energy (ZPE) contributions were not included because ZPE could not be evaluated for those systems where intermolecular constraints were applied.

## Results and Discussion

Intermolecular complex of cation **b** with benzene comprises three distinct structural units, such as a benzenium cation (**A**), a propylene molecule (**B**), and the reactant benzene molecule (**C**). Each component has already been subjected to detailed quantum chemical studies.<sup>35–39</sup> Their gas-phase homodimers<sup>40–44</sup> and heterodimers<sup>21,22,45,46</sup> with various small molecules are documented in the literature as well. However, neither the **A**–**C** and **B**–**C** pairs nor the trimolecular complex formed by the cooperation of **A**, **B**, and **C** have been described yet. Although there is a broad variety of the possibilities of how to arrange parts **A**, **B**, and **C** in the space, in this work we will characterize only those structures that are important from the catalytic point of view.

**Proposed Structure of the Initial State Complexes.** At first, a full-geometry optimization was performed on the complex of cation **b** and benzene that led to the result presented as structure **1** (see structures). The total HF/6-31G\*\* energies

CHART 1

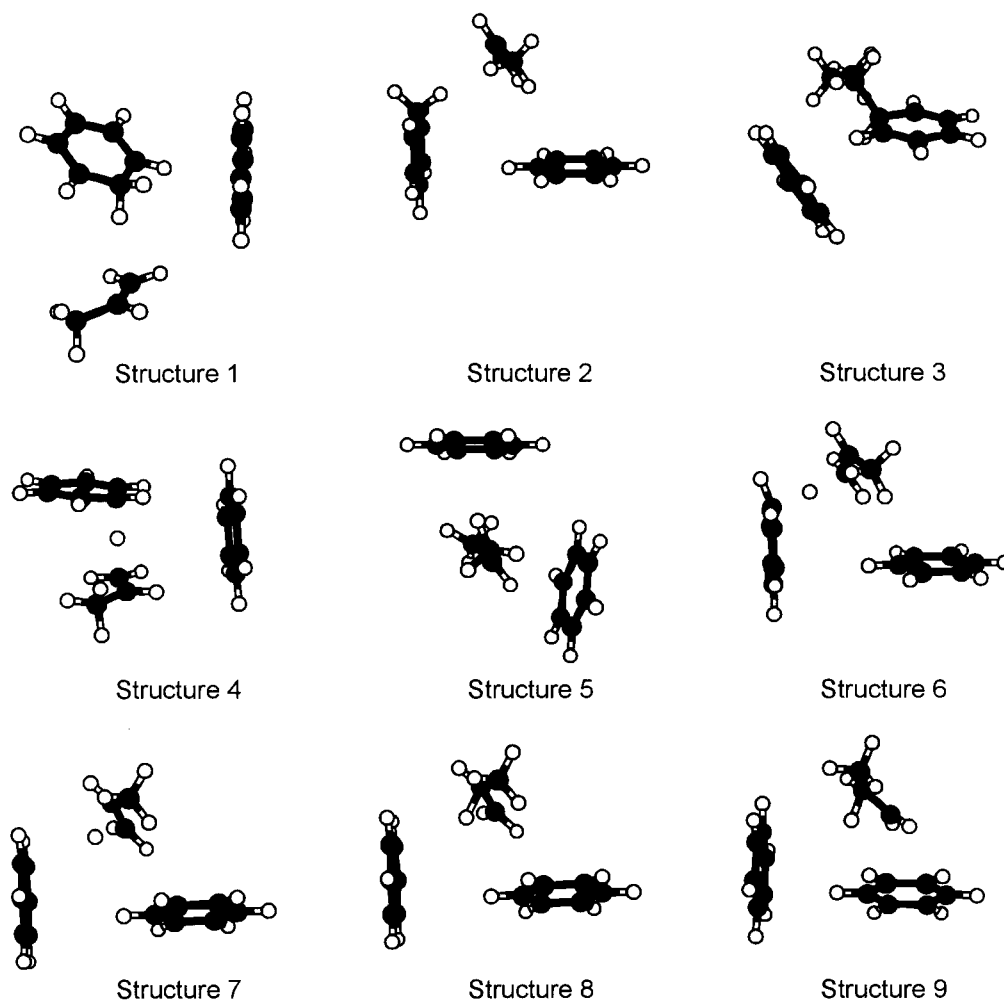


**TABLE 1: Total Electronic Energies (HF/6-31G\*\* Level) and Interaction Energies (MP2/6-31G\*(0.25)/HF/6-31G\*\*) of the Complexes Obtained from Ab Initio Quantum Chemical Calculations<sup>a</sup>**

structure	$E^{\text{tot}}$	$E^{\text{tot'}}$	$\Delta E^{\text{AB}}$	$\Delta E^{\text{AC}}$	$\Delta E^{\text{BC}}$	$\Delta E^3$
1	-578.838 995 2	0.0	-5.5	-9.1	-0.3	0.4
2	-578.830 964 6	+5.0	-5.8	-1.5	-1.2	0.0
3 <sup>b</sup>	-578.863 082 2	-15.1	-9.2			
4 <sup>c</sup>	-578.812 098 2	+16.9	-8.3			
5	-578.849 351 5	-6.5	-10.3	-0.3	-14.4	1.1
6 <sup>c</sup>	-578.803 891 8	+22.0	-4.7			
7	-578.824 963 3	+8.8	-9.8	-1.2	-8.1	0.9
8	-578.821 058 6	+11.3	-9.3	-1.2	-8.5	0.8
9	-578.821 516 7	+11.0	-6.9	-1.9	-13.8	0.6

<sup>a</sup>  $E^{\text{tot}}$  = total energy (in au);  $E^{\text{tot'}}$  = total energy relative to that of structure 1 (kcal/mol);  $\Delta E^{\text{AB}}$ ,  $\Delta E^{\text{AC}}$ ,  $\Delta E^{\text{BC}}$  designate the bimolecular pair additive terms of the interaction energy (in kcal/mol);  $\Delta E^3$  = three-body term (kcal/mol). <sup>b</sup> In this structure, the propylene (B) and benzene (C) parts are non-separable; therefore, the interaction energy has been computed between parts A and B + C. <sup>c</sup> In this structure, the arenium (A) and propylene (B) parts are non-separable; therefore, the interaction energy has been computed between parts A + B and C.

and MP2/6-31G\*(0.25) interaction energies are given in Table 1 (row 1) for this structure. The interaction energies indicate that the major portion of the stabilization of the complex (9.1 kcal/mol) comes from the interaction between parts A and C. Interaction between the arenium and propylene parts contributes to the total stabilization energy to a lesser extent (by 5.5 kcal/mol). Interaction between the benzene and propylene parts as well as the three-body term are negligible.

The geometry of structure 1 can be discussed in terms of the stabilization effects already described. The relative position of the benzene rings in structure 1 closely resembles the optimized structure of the complex formed by interaction between the isopropyl carbocation and benzene.<sup>21</sup> The benzenium cation is oriented to the center of the benzene ring through the  $\text{sp}^2$  carbon adjacent to the  $\text{sp}^3$  carbon of the protonated ring. The axis of the arenium part is declined by  $60^\circ$  from the plane of the benzene ring that is very close to the corresponding value obtained at HF level of theory on the same basis set for the complex of isopropyl carbocation and benzene ( $54^\circ$ ). Let us note, however, that due to the steric conditions present at the channel intersection of zeolites of MFI and MEL structural types, accommodation of structure 1 would require placing the protonated part of the complex into the sinusoidal channels that is (as already shown) less likely.

Structure 1 is the result of a full optimization, therefore it can be formed on open surfaces or in large pore media only where no steric restrictions can hinder the system to achieve the minimum energy atomic configuration. Nevertheless, no catalytic activity is associated with the nonrestricted reaction space,<sup>7,8</sup> indicating that the intermediate of the reaction responsible for the *n*-propylbenzene formation must be different from structure 1. Experimental studies indicate the structure-directing role of the narrow perpendicular intersecting channels of zeolites of the MFI and MEL structural types. Consequently, a model system was considered that reflects the geometrical constraints defined by the perpendicular intersecting channels in zeolites

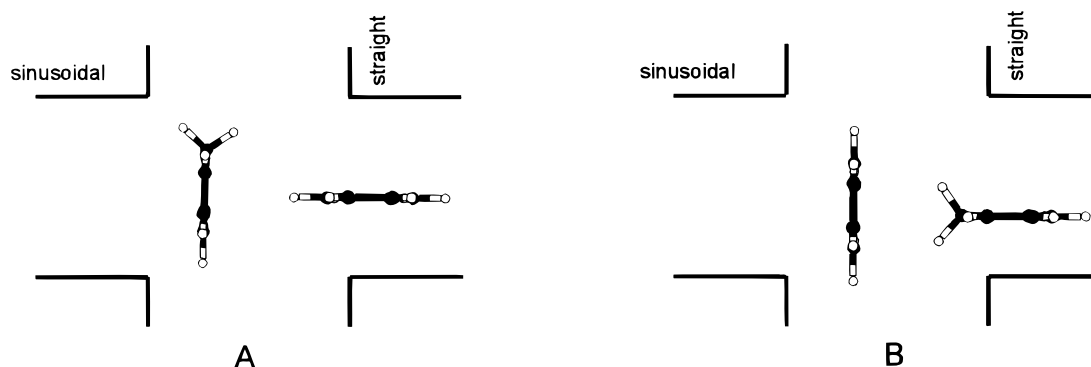


**Figure 1.** Possible mutual positions of the arenium (A) and benzene (C) parts of the reaction complex embedded into the intersection of the straight and sinusoidal channels of zeolites of the MFI and MEL structural types.

of the MFI and MEL structural types. In fact, as shown in Figure 1, perpendicular position for the benzenium cation and benzene molecule inside the MFI or MEL structures can be achieved in two different ways: by placing either the benzenium cation (Figure 1A) or the benzene (Figure 1B) into the channel intersections. Nevertheless, based on the arguments mentioned in the *Introduction*, we focused our attention on the first possibility.

Structure 2 represents the optimized geometry of the complex of benzenium cation, propylene, and benzene obtained with restricting the perpendicular position of the 2-fold rotation axes of the six-membered rings. A comparison of the computed total energies (see Table 1) shows that structure 2 is  $\sim 5$  kcal/mol less stable than structure 1. This energy difference can be unambiguously assigned to the lack of the stabilization derived from the interaction of parts A and C because all other energy terms are practically the same for both structures. Therefore, the major effect of the geometrical constraints imposed is the separation of the arenium part and the benzene ring.

**Proposed Structure of the Product.** The isomerization reaction of isopropylbenzene to *n*-propylbenzene can be considered as a transalkylation reaction between cation **b** and benzene. The reaction is initialized by the displacement of the proton from the  $sp^3$  carbon of the benzenium cation toward part B. According to the Markovnikov rule, addition of a proton to the propylene molecule can be expected at its primary carbon atom because of the pronounced stability of the secondary isopropyl carbocation formed. In principle, formation of *n*-propyl group by the protonation of propylene requires an energetically less favored *anti*-Markovnikov-type reaction route. However, in the MFI and MEL structures, this pathway is strongly supported by experimental studies. To explore the role of the zeolite matrix in the *anti*-Markovnikov-type proton addition, an attempt was made to determine the structure of a complex of two benzene molecules and an *n*-propyl carbocation, where the initial position of the six-membered rings (parts A and C) has been taken from Structure 2. No local minimum was found for this system. Instead, the *n*-propyl group forms a covalent bond with one of the benzene rings, directly resulting in a bimolecular complex of *n*-propylbenzene and benzene [i.e., the assumed primary product of the reaction (*vide infra*)].

The optimized geometry of the primary (protonated) product of the isomerization reaction obtained with full relaxation of all parameters is depicted by structure 3. Because the structure is compact, no constraints were necessary to apply to model the steric effect of the zeolite matrix. The total energy of this structure is 20 kcal/mol lower than that of structure 2. This substantial stabilization can evidently be attributed to the formation of a chemical bond between parts B and C. The

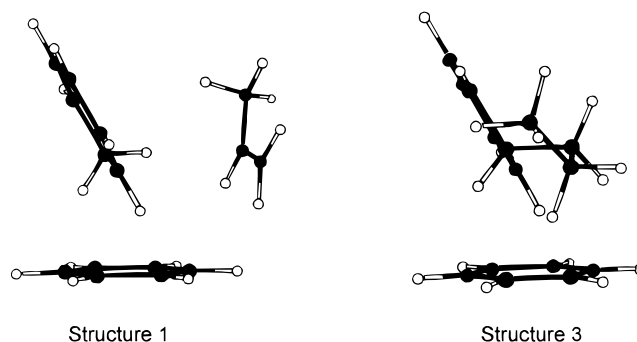


**Figure 2.** Similarity between the computed geometries of structures 1 and 3.

corresponding data of Table 1 indicate a similar interaction between the arenium part and the benzene molecule in structures 1 and 3. Figure 2 illuminates the origin of the close similarity between structures 1 and 3 using another projection. It can be seen that the relative orientation of the arenium part and benzene is practically the same in both complexes. Moreover, it is interesting to note that both complexes are centered at the benzene ring through the carbon adjacent to the  $sp^3$  carbon of the benzenium cation, which is in agreement with the generally known rule that protonation of an aromatic system produces a local positive charge on the neighboring carbon atom.

Although structure 3 possesses a slightly more compact global structure than structure 2, it can be formed in the zeolite channels only in one particular case; namely, when the *n*-propyl group is attached to part C of structure 2. The upper model of Figure 3 shows structure 2 embedded in the intersection of the perpendicular channels of the MFI and MEL zeolites. Below, variants "A" and "B" represent the two possibilities for the accommodation of the primary product (structure 3) obtained via chemical bond formation between parts B and C or parts A and B of structure 2, respectively. It can be clearly seen that only variant "A" can stand for the real situation because variant "B" would imply a large displacement of the benzene ring (part C) localized in the sinusoidal channels on the opposite side of the complex that is hindered by the matrix. In contrast, variant "A" can be easily obtained from the initial state complex (see the upper model in Figure 3) by a relatively small displacement of part A of structure 2. These arguments support the experimental observation, as in the perpendicular channel system of the MFI and MEL structures, that *n*-propylbenzene can be formed exclusively via a *bimolecular* pathway.

***n*-Propylbenzene Is Not Formed for Unconstrained Structure.** As already discussed, the experimental results show no *n*-propylbenzene formation on open surfaces or in zeolites with large cavities. This result might be surprising because structures



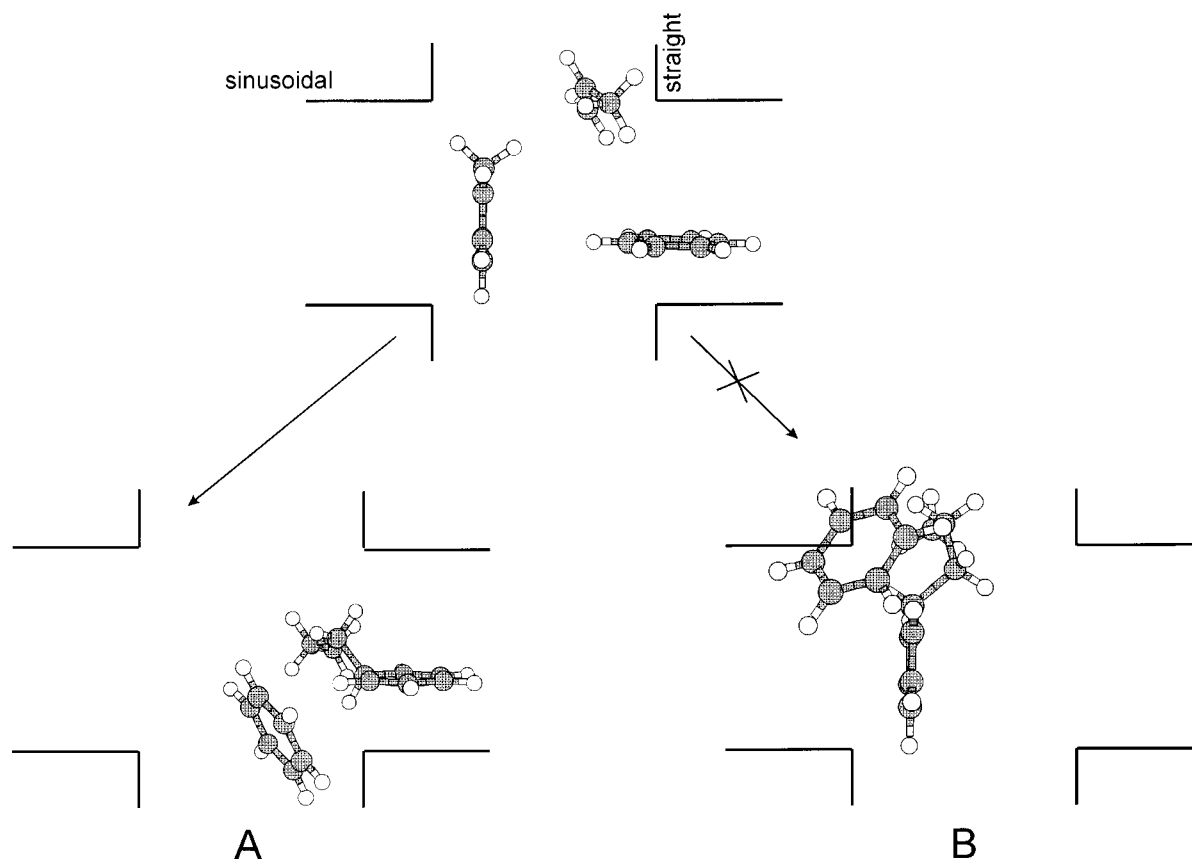


**Figure 3.** Steric conditions for the accommodation of the expected primary product of the isomerization reaction in the MFI and MEL matrixes.

**1** and **3** are geometrically very close to each other, which could suggest the presence of a reaction pathway between them. To clarify this point, we tried to follow the fate of structure **1**, choosing the bond distance between the  $sp^3$  carbon of the arenium part and the bridging hydrogen as the reaction coordinate. Geometry optimizations were performed with various fixed  $C\cdots H$  distances within the range of 1.1 to 3.0 Å. The rate-determining step (barrier) was found at a bond distance of 1.45 Å, with the gas-phase activation energy of 16.9 kcal/mol. Let us note that the activation energies for proton-transfer processes are known to be overestimated by the HF/6-31G\*\* approximation.<sup>47</sup> This step can be assigned to the removal of the proton from the  $sp^3$  carbon of the benzenium cation, which initializes a substantial reorganization of the reaction center illustrated by structure **4**. A comparison between structures **1** and **4** obviously shows that the proton loss of the benzenium part (and simultaneously the protonation of the double bond in part **B**) involves a substantial displacement of part **C** toward part **B**. Computed interaction energies indicate a strong attraction (8.3 kcal/mol) between part **C** and the remainder of the complex, which can be unambiguously associated with the interaction between parts **B** and **C** because the benzenium and the benzene parts are fairly separated in space. Further displacement of the proton does not result in a substantial change of the global structure and eventually leads to the formation of a complex containing an isopropyl carbocation surrounded by two benzene rings (structure **5**). Therefore, this reaction pathway does not lead to *n*-propylbenzene formation.

**Instability of the *n*-Propyl Carbocation.** As already shown, the one-dimensional search on the potential energy hypersurface for the unconstrained structure leads to the arrangement where the isopropyl cation is buried by two benzene rings. This result indicates that the isopropyl cation is stabilized as an ionic species

in this environment. For comparison, we made an attempt to optimize the corresponding structure containing the *n*-propyl cation. No such minimum was found, because the *n*-propyl cation isomerizes back to the isopropyl cation without changing the global structure. Based on the arguments just made, formation of *n*-propyl carbocation stabilized by two interacting benzene rings (that can be considered as the precursor of *n*-propylbenzene) is not the favored pathway in this mechanism.

Let us summarize that in accordance with the general opinion, *n*-propyl carbocation was unstable in both model systems considered in this study. It is interesting to note that the reason for destabilization of the *n*-propyl carbocation is strongly influenced by the relative spatial arrangement of the benzene rings. In the fully relaxed structure, the *n*-propyl carbocation isomerizes to the more stable isopropyl cation, whereas the covalent bond formation in a concerted reaction (yielding *n*-propylbenzene) is the preferred pathway when the relative position of the benzene rings is constrained (vide infra).

**Route to *n*-Propylbenzene—The Steric Effect of the Zeolite Matrix.** The activation energy of the isomerization reaction was estimated on the constrained model by evaluating a single proton-transfer pathway from the  $sp^3$  carbon of the benzenium carbocation. The barrier was localized near the distance of 1.45 Å from the  $sp^3$  carbon of the arenium part. To simulate the effect of the zeolite matrix, the relative position of the benzene rings was adopted from structure **2**, and only the rotation of the benzene rings was permitted. The computed energy barrier is roughly the same (17.0 kcal/mol) as obtained when no geometrical restrictions have been imposed. The geometry of the transition complex is depicted by structure **6**. Obviously, the geometrical restriction imposed for the relative position of the benzene rings prevails over the global structure of the transition complex. Although structure **1** underwent consider-

able changes upon removal of the proton from the arenium part (for comparison see structure 4), the main features of the initial state (represented by structure 2) are preserved in structure 6. A comparison between structures 4 and 6 shows that the relative spatial position of parts B and C is fairly different in the constrained and unconstrained transition state structures. For illustration, we calculated the averaged value of the interatomic distances between part C and the primary and secondary carbon atoms of part B, respectively. In structure 4, the primary and secondary carbon atoms both are centered at the benzene ring. The averaged interatomic carbon-carbon distances are 4.51 and 4.53 Å for the secondary and primary carbons of the propylene part, respectively. In contrast, in structure 6, part B has only three contacts with the benzene rings because all other distances considered are longer than 5.0 Å. The averages obtained, including only those contacts that are closer than 5.0 Å, are 4.19 and 4.75 Å for the primary and secondary carbons, respectively. Obviously, the steric conditions for the *n*-propylbenzene formation are better in structure 6 than in structure 4. In agreement with this result, two possible ways arise for the stabilization of the reaction complex embedded in the MFI and MEL structures. (i) A Markovnikov-type reaction route leads to a complex of isopropyl carbocation surrounded by two perpendicular benzene rings. This route is the analogue of the reaction pathway presented for the nonrestricted reaction volume. (ii) The calculations have revealed the existence of an anti-Markovnikov-type reaction route as well. Structures 7, 8, and 9 demonstrate the representative points along this pathway. Structure 7 can be considered as a complex of protonated propylene and two perpendicular benzene molecules where the proton occupies the bridging position between the primary and secondary carbon of part B. This model was obtained from an optimization where (beyond the parameters used for the description of the steric effect of the matrix) the position of the bridging proton was localized in the perpendicular plane located in the middle of the double bond of the propylene (part B). The optimal C-H bond distance for the bridging proton was found at 1.31 Å. The possibility of an anti-Markovnikov-type proton addition was evaluated starting from this structure by fixing the bond distance between the bridging proton and the secondary carbon of part B at 1.20 (structure 8) and 1.15 Å (structure 9). The corresponding total energy data of Table 1 show that formation of structures 7, 8, and 9 is energetically accessible because they are more stable than the activated complex (structure 6). Therefore, a sequence of structures 2, 6, 7, 8, 9, and 3 can describe a possible route leading to the *n*-propylbenzene formation.

## Conclusions

In agreement with the experimental results, the computations support a proton-catalyzed bimolecular pathway for the isomerization reaction of isopropylbenzene leading to *n*-propylbenzene. The term "structure-directed transition state selectivity" (see ref 6) comprises two important aspects of the reaction mechanism:

(i) In contrast to the isopropyl carbocations, *n*-propyl carbocations cannot be stabilized by two interacting benzene molecules under the geometrical conditions considered in this study. The architecture and dimensions of the matrix are the dominant factors in determining the fate of the *n*-propyl carbocation. Our calculations have shown that in nonrestricted reaction space, the *n*-propyl carbocations readily isomerize to isopropyl carbocations. On the other hand, in the perpendicular channel system of the MFI and MEL structures, the chemical

bond formation between the *n*-propyl group and benzene becomes the way of stabilization.

(ii) The primary product of the reaction inside the MFI and MEL structures is a complex of protonated *n*-propylbenzene and benzene. Because of the steric restrictions, the product can be stabilized only in the case when the *n*-propyl group is attached to the benzene ring localized in the sinusoidal channels supporting a bimolecular pathway.

Based on the computational results, the main steps of the proton-catalyzed bimolecular mechanism can be summarized as follows. In a preceding step of the reaction, the protonated isopropylbenzene molecules adsorbed at the channel intersections undergo an attack by the benzene molecules diffusing through the sinusoidal channels and form the intermediate complex shown by structure 2. The isomerization reaction is initialized by the transfer of the bridging hydrogen from the sp<sup>3</sup> carbon of the arenium part toward the propylene part. The anti-Markovnikov-type proton addition to the propylene part is promoted by the formation of covalent bond between the reactant benzene molecule and the propylene part that results in a substantial stabilization of the complex.

**Acknowledgment.** This work was supported by the Academy of Sciences of the Czech Republic (Grant No. A4040707). Assistance of Mrs. N. Žilková in preparation of the figures is greatly acknowledged.

## References and Notes

- (1) Kaeding, W. W. *J. Catal.* **1985**, *95*, 512.
- (2) Fraenkel, D.; Levy, M. *J. Catal.* **1989**, *118*, 10.
- (3) Beyer, H. K.; Borbély, G. In *Proceedings of the 7th Int. Conf. Zeol.; Kodansha-Elsevier*: Tokyo, 1987; p 867.
- (4) Ivanova, I. I.; Brunel, D.; Nagy, J. B.; Daelen, G.; Derouane, E. G. *Stud. Surf. Sci. Catal.* **1993**, *78*, 587.
- (5) Ivanova, I. I.; Brunel, D.; Nagy, J. B.; Derouane, E. G. *J. Mol. Catal. A: Chemical* **1995**, *95*, 243.
- (6) Wichterlová, B.; Čejka, J. *J. Catal.* **1994**, *146*, 523.
- (7) Čejka, J.; Vondrová, A.; Wichterlová, B.; Vorbeck, G.; Fricke, R. *Zeolites* **1994**, *14*, 147.
- (8) Čejka, J.; Kapustin, A. G.; Wichterlová, B. *Appl. Catal. A: General* **1994**, *108*, 187.
- (9) Wichterlová, B.; Čejka, J.; Žilková, N. *Microporous Mater.* **1996**, *6*, 405.
- (10) Jentys, A.; Lercher, J. A. In *Zeolites as Catalysts, Sorbents and Detergent Builders*; Elsevier: Amsterdam, 1989; p 585.
- (11) Jentys, A.; Warecka, G.; Lercher, J. A. *J. Mol. Catal.* **1989**, *51*, 309.
- (12) Mirth, G.; Čejka, J.; Lercher, J. A. *J. Catal.* **1993**, *139*, 24.
- (13) Teunissen, E. H.; van Santen, R. A.; Jansen, A. P. J.; van Duijneveldt, F. B. *J. Phys. Chem.* **1993**, *97*, 203.
- (14) Blaszkowski, S. R.; van Santen, R. A. *J. Am. Chem. Soc.* **1997**, *119*, 5020.
- (15) Jobic, H.; Tuel, A.; Krossner, M.; Sauer, J. J. *Phys. Chem.* **1996**, *100*, 19545.
- (16) Boronat, M.; Viruela, P.; Corma, A. *J. Phys. Chem.* **1996**, *100*, 633.
- (17) Xu, T.; Haw, J. F. *J. Am. Chem. Soc.* **1994**, *116*, 10188.
- (18) Kazansky, V. B.; Senchenya, I. N. *Catal. Lett.* **1991**, *8*, 317.
- (19) Pelmenshikov, A. G.; Žhanpeisov, N. U.; Paukshts, E. A.; Malysheva, L. V.; Zhidomirov, G. M.; Zamaraev, K. I. *Dokl. Akad. Nauk SSSR* **1987**, *293*, 915.
- (20) Demidov, A. V.; Davydov, A. A. *Mater. Chem. Phys.* **1994**, *39*, 13.
- (21) Berthomieu, D.; Brenner, V.; Ohanessian, G.; Denhez, J. P.; Millié, P.; Audier, H. E. *J. Am. Chem. Soc.* **1993**, *115*, 2505.
- (22) Berthomieu, D.; Brenner, V.; Ohanessian, G.; Denhez, J. P.; Millié, P.; Audier, H. E. *J. Phys. Chem.* **1995**, *99*, 712.
- (23) Derouane, E. G.; Gabelica, Z. *J. Catal.* **1980**, *65*, 486.
- (24) Schlegel, H. B. *J. Comput. Chem.* **1982**, *3*, 214.
- (25) Hobza, P.; Šponer, J.; Reschel, T. *J. Comput. Chem.* **1995**, *16*, 1315.
- (26) Kristián, S.; Pulay, P. *Chem. Phys. Lett.* **1994**, *239*, 175.
- (27) Kroon-Battenburg, L. M. J.; Van Duijneveldt, F. B. *J. Mol. Struct.* **1985**, *121*, 185.
- (28) Hobza, P.; Šponer, J.; Polasek, M. *J. Am. Chem. Soc.* **1995**, *117*, 792.

- (29) Šponer, J.; Leszczynski, J.; Hobza, P. *J. Phys. Chem.* **1996**, *100*, 5590.
- (30) Šponer, J.; Hobza, P. *Chem. Phys. Lett.* **1997**, *267*, 263.
- (31) Hobza, P.; Šponer, J.; Leszczynski, J. *J. Phys. Chem.* **1997**, *101*, 8083.
- (32) Burda, J.; Šponer, J.; Leszczynski, J.; Hobza, P. *J. Phys. Chem.* **1997**, *101*, 9670.
- (33) These values can be corrected by adding the correlation component of the MP2/6-31G\*(0.25)//HF/6-31G\*\* interaction energies which would basically include the effect of the dispersion attraction.
- (34) Frisch, M. J.; Trucks, G. W.; Schlegel, H. B.; Gill, P. M. W.; Johnson, B. G.; Robb, M. A.; Cheeseman, J. R.; Keith, T.; Petersson, G. A.; Montgomery, J. A.; Raghavachari, K.; Al-Laham, M. A.; Zakrzewski, V. G.; Ortiz, J. V.; Foresman, J. B.; Cioslowski, J.; Stefanov, B. B.; Nanayakkara, A.; Challacombe, M.; Peng, C. Y.; Ayala, P. Y.; Chen, W.; Wong, M. W.; Andres, J. L.; Replogle, E. S.; Gomperts, R.; Martin, R. L.; Fox, D. J.; Binkley, J. S.; Defrees, D. J.; Baker, J.; Stewart, J. P.; Head-Gordon, M.; Gonzalez, C.; Pople, J. A. *Gaussian 94*; Gaussian, Inc.: Pittsburgh, PA, 1995.
- (35) Peck, R. C.; Schulman, J. M.; Disch, R. L. *J. Phys. Chem.* **1990**, *94*, 6637.
- (36) Maslen, P. E.; Handy, N. C.; Amos, R. D.; Jayatilaka, D. *J. Chem. Phys.* **1992**, *97*, 4233.
- (37) Howard, S. T.; Wozniak, K. *Chem. Phys. Lett.* **1993**, *212*, 1.
- (38) Durig, J. R.; Guirgis, G. A.; Bell, S. *J. Phys. Chem.* **1989**, *93*, 3487.
- (39) Dahlke, G. D.; Kass, S. R. *J. Am. Chem. Soc.* **1991**, *113*, 5566.
- (40) Hobza, P.; Selzle, H. L.; Schlag, E. W. *J. Chem. Phys.* **1990**, *93*, 5893.
- (41) Henson, B. F.; Hartland, G. V.; Venturo, V. A.; Felker, P. M. *J. Chem. Phys.* **1992**, *97*, 2189.
- (42) Hobza, P.; Selzle, H. L.; Schlag, E. W. *J. Am. Chem. Soc.* **1994**, *116*, 3500.
- (43) Jaffe, R. L.; Smith, G. D. *J. Chem. Phys.* **1996**, *105*, 2780.
- (44) Hiraoka, K.; Fujimaki, S.; Aruga, K.; Yamabe, S. *J. Chem. Phys.* **1991**, *95*, 8413.
- (45) Xu, L.-W.; Kuczkowski, R. L. *J. Chem. Phys.* **1994**, *100*, 15.
- (46) Taleb-Bendiab, V.; Hillig II, K. W.; Kuczkowski, R. L. *J. Chem. Phys.* **1992**, *96*, 2996.
- (47) Florian, J.; Leszczynski, J. *J. Am. Chem. Soc.* **1996**, *118*, 3010